Compact and self-aligned all-optical image correlator based on third-harmonic generation

Shuo-Yen Tseng, Canek Fuentes-Hernandez, and Bernard Kippelen*

Center for Organic Photonics and Electronics, School of Electrical and Computer Engineering, Georgia Institute of Technology, Atlanta, Georgia 30332, USA
**Corresponding author: kippelen@gatech.edu*

Received July 2, 2007; revised August 1, 2007; accepted August 1, 2007; posted August 6, 2007 (Doc. ID 84720); published August 24, 2007

We demonstrate a compact optical correlator using a diffractive optical element (DOE) beam splitter for 2D optical image processing. Image frequency conversion and correlation are demonstrated using third-harmonic generation (THG) in an organic film with a 1550 nm femtosecond laser. Spatial and temporal alignment of the femtosecond pulses are obtained by imaging the DOE onto the organic film. © 2007 Optical Society of America

OCIS codes: 070.4550, 070.4340, 120.4570.

All-optical processors are attractive for computationally intensive tasks such as 2D image correlation [1]. In particular, Fourier-transform-based image correlators have many important applications, such as pattern recognition. The recent advance of novel nonlinear optical (NLO) materials [2,3] allows the realization of dynamic image correlations on a fast time scale utilizing the large third-order nonlinear susceptibilities in these materials. Since third-order nonlinear susceptibilities are orders of magnitude lower than second-order ones, high-intensity lasers with subpicosecond pulses are generally required for these correlator systems. The need of beam steering optics and temporal delay lines to obtain good spatial and temporal overlap of the interacting pulses makes these systems bulky, prone to misalignment, and hard to implement outside of a laboratory environment. An attractive alternative to beam steering optics is to use diffractive optical element (DOE) beam splitters. It has been demonstrated by several groups that relatively simple and easy to align setups can be built for various transient grating [4,5] and four-wave mixing [6] experiments utilizing subpicosecond pulses with DOE beam splitters. These systems generally require fewer optical elements than their counterparts using beam steering optics. Therefore, the potential benefits of DOE-based optical correlators are their compact size, robustness, and ease of alignment. In this Letter, we demonstrate a compact optical setup that uses a DOE beam splitter for the implementation of a matched filter type optical correlator based on the third-harmonic generation (THG) approach shown in Fig. 1.

In this compact optical correlator, the input beam is focused to a spot on the DOE beam splitter, which splits the input beam into four $(\pm 1, \pm 1)$-order beams. The DOE is similar to the 2D phase grating with 40 μm periods in both directions used in [6], which is designed to optimize the diffraction efficiency into the $(\pm 1, \pm 1)$ orders at 1550 nm for coherent detection of the degenerate four-wave mixing (DFWM) signal in a folded crossed-beam phase-matched coherent anti-Skokes Raman spectroscopy (BOXCARS) geometry [7]. Due to fabrication imperfections, the DOE diffracts 10% of the input energy into each of the $(\pm 1, \pm 1)$-order beams. The diffracted beams are collimated with a $f_1 = 15$ cm focal length spherical lens. Three of the four $(\pm 1, \pm 1)$-order beams are picked with a beam block containing the binary images used as transmission masks for the correlation experiments. The position of the block defines the first Fourier plane of a 4-*f* imaging system, which proceeds as follows: images inserted into the beam paths are Fourier transformed by a $f_2 = 10$ cm focal length lens focused onto the NLO sample. The images mix inside the NLO sample via its third-order susceptibility, which, in this case, is the THG characterized by $\chi^{(3)}(3\omega; \omega, \omega, \omega)$. The beam crossing angles are 6.6° between beams 1, 3, and 4.7° between beams 1, 2 and 2, 3. A second $f_3 = 10$ cm focal length lens is placed behind the NLO sample to Fourier transform the nonlinear correlation signal generated by wave mixing onto the image plane, where the signal is captured by an Si CCD camera (GENWAC, GW-902H). The use of

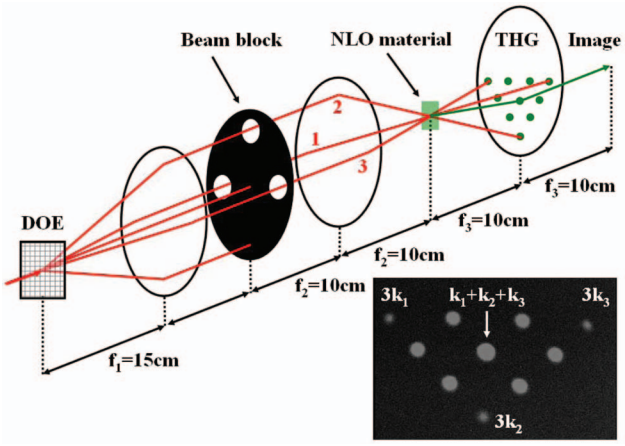

Fig. 1. (Color online) Schematic of the compact optical correlator using a DOE beam splitter. The DOE is a 2D phase grating with 40 μm periods in both directions. Images for processing are inserted into the beam paths of the three $(\pm 1, \pm 1)$ order beams picked by the beam block. The inset shows the ten generated THG beams captured by an Si CCD camera. The center THG beam, $\mathbf{k}_1 + \mathbf{k}_2 + \mathbf{k}_3$, is used for correlation.

0146-9592/07/172599-3/$15.00

a DOE beam splitter ensures both the spatial and temporal overlap of the interacting beams when they are focused onto the NLO sample. Moreover, the DOE beam splitter also allows the overlap of short pulses over their full aperture [8] inside the NLO sample, since the phase fronts of the diffracted beams travel parallel to one another. The entire correlator setup was implemented on a small breadboard (10 cm × 60 cm) and required minimal alignment. We also point out that all the lenses used in the setup were low-cost commercially available singlet plano–convex spherical lenses, which provided a maximum resolution of 14.30 lines/mm at the fundamental wavelength tested using a standard U.S. Air Force (USAF) resolution target.

For our experiment, we have used the same 10 μm thick polymer composite film used for the demonstration of the THG-based optical signal processing experiments reported elsewhere [9–12]. The laser source was an ultrafast optical parametric amplifier (Newport TOPAS) pumped by a Ti:sapphire regenerative amplifier (Newport Spitfire) producing 100 fs pulses at $\lambda = 1550$ nm with a repetition rate of 1 kHz. The pulse energy in each of the diffracted $(\pm 1, \pm 1)$ orders was 2.8 μJ/pulse. When the pulses in the three $(\pm 1, \pm 1)$-order beams at frequency ω are spatially and temporally overlapped on the NLO sample, ten THG beams at 3ω can be observed in different directions as expected from the vectorial combinations of the wave vectors of the three interacting beams. These ten THG beams were captured with the CCD camera as shown in the inset of Fig. 1. Directions of these beams are also shown in the same figure, where $\mathbf{k}_1$, $\mathbf{k}_2$, and $\mathbf{k}_3$ are the wave vectors of the fundamental beams at ω. The middle THG beam in the direction of $\mathbf{k}_1+\mathbf{k}_2+\mathbf{k}_3$ is generated with one photon from each of the fundamental beams, therefore producing a spatial amplitude $A_{\mathrm{THG}}(r')$ at the image plane proportional to

$$A_{\mathrm{THG}}(r') \propto A_1(r) \otimes A_2(r) \otimes A_3(r), \qquad (1)$$

where $\otimes$ denotes convolution, and A_i's are the images encoded in the fundamental beams. The spatial coordinates r' and r are related as $r' = 3(f_1/f_2)r$, where the factor 3 appears because $\lambda_{\mathrm{THG}} = \lambda/3$ [13].

In Eq. (1), when two of the fundamental images are the delta function, $\delta(r)$, the spatial amplitude of the THG signal is proportional to the image encoded in the third fundamental beam. In the experiments, we encoded points of various diameters in the beams to simulate the delta function. First, points were encoded in beams 1 and 3, and 3.5 mm × 3.5 mm letters were encoded in beam 2 by inserting images printed on transparencies. The 3ω image in the middle THG beam, $\mathbf{k}_1+\mathbf{k}_2+\mathbf{k}_3$, was spatially selected with an iris and captured at the image plane with the Si CCD camera. In Fig. 2, frequency converted letters generated with 1.0 mm [Fig. 2(a)] and 0.5 mm [Fig. 2(b)] diameter points are shown for comparison. The finite size of the points encoded in the beams limits the extents of the sampled spectral components in the Fourier plane (NLO sample plane); as a result, the resolution of the frequency converted images is limited. It is clear that the smaller the points are, the better the resolution is at the image plane. However, the throughput power in these beams will be reduced as a consequence of the reduced point sizes. We also tested the correlator with airplane images, which were later used in the correlation experiments. Figure 3 shows the results of image frequency conversion with 0.5 mm diameter points.

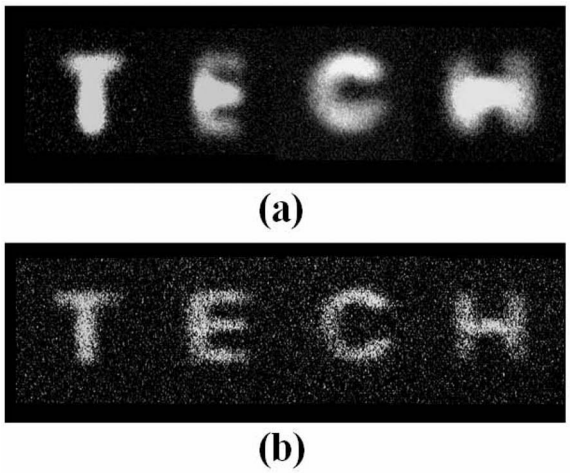

Fig. 2. Frequency converted letters taken at the image plane with an Si CCD camera. Using points to simulate the delta function in beams 1 and 3, images were encoded in beam 2 at frequency ω and frequency converted to 3ω using THG in an organic film. Better resolution was obtained when the points better approximated the delta function. Diameter of the points: (a) 1.0 mm, (b) 0.5 mm.

For image correlation, a 0.5 mm diameter point was encoded in beam 1. In beam 3, an airplane inverted about its own origin [Fig. 4(a)] was encoded as the target. From Eq. (1), it can be seen that the THG signal is approximately the convolution of images 2 and 3, that is, $A_{\mathrm{THG}}(r') \approx A_2(r) \otimes A_3(r)$. To obtain the

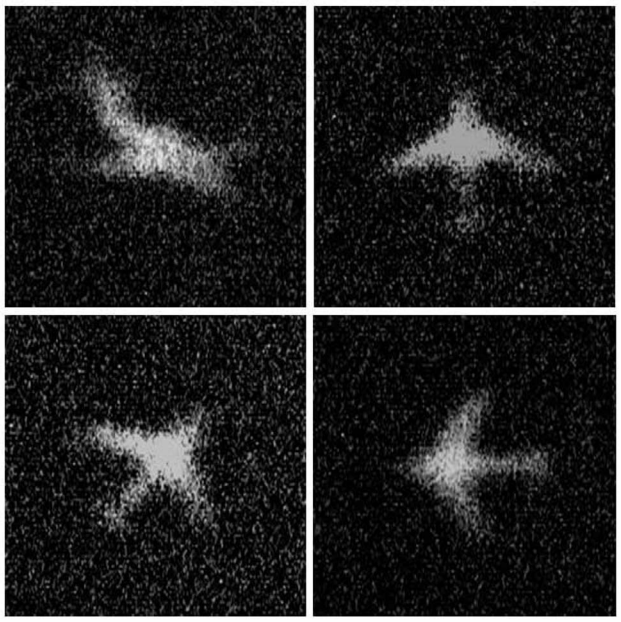

Fig. 3. Frequency converted images of an aircraft using 0.5 mm diameter points in beams 1 and 3.

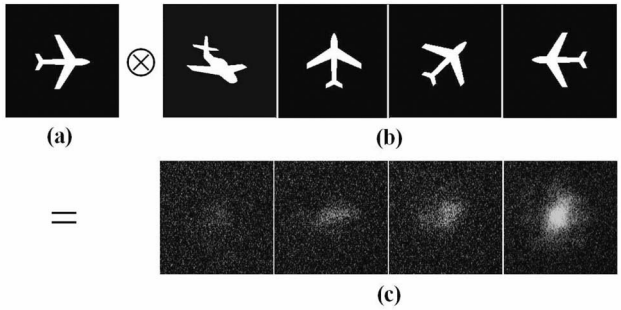

Fig. 4. Inverted target image (a) in beam 1 and input images (b) in beam 2 used for the correlation experiment. The corresponding correlation results are shown in (c). ⊗ denotes convolution.

cross correlation of the target image and input images, the target image has to be inverted about its own origin [1]. Images shown in Fig. 4(b) [the same images used for frequency conversion shown in Fig. 3] were encoded in beam 2, and their correlation results with the target image in the center THG beam are shown in Fig. 4(c). A clear autocorrelation peak can be observed when the input image matches the target image. The correlation between the target airplane and the rotated airplanes are reduced, showing rotational variance of the correlation. Again, the resolution is limited by the diameter of the point encoded in beam 1.

In the current correlator setup, only 10% of the input laser energy is diffracted into each of the interacting beams; a better fabricated and designed DOE beam splitter will greatly improve the efficiency of future systems. The THG conversion efficiency can also be optimized by changing the beam crossing angle and beam pattern on the NLO sample to obtain better phase matching [12] between the fundamental and the THG frequencies. The resolution is limited by the use of small diameter points to simulate the delta function in Eq. (1) while maintaining enough energy in the beams for the nonlinear process. This limitation can be circumvented by focusing the beams onto the front focal plane of the second lens in Fig. 1. However, care must be taken to compensate for the path-length difference introduced by the insertion of lenses.

In conclusion, we have demonstrated a compact optical correlator using a DOE beam splitter for all-optical image correlation using third-order nonlinear effects in NLO materials with 100 fs pulses at 1550 nm. Image frequency conversion and correlation were demonstrated with this system using THG in a NLO sample. Spatial and temporal overlap of the pulses were obtained with relative ease by imaging the DOE onto the NLO sample. The use of a DOE beam splitter greatly reduces the complexity and size of the correlator, which makes the correlator portable, robust, easy to align, and potentially useful outside of a laboratory environment.

The authors thank J. Goldhar and W. N. Herman for generously providing the DOE used in the experiments, S. R. Marder and his group for providing the organic NLO chromophores for the THG experiments, and J. W. Perry and his group for letting us use their femtosecond laser system. This work was funded in part by NSF through STC DMR-0120967 and by a Defense Advanced Research Projects Agency (DARPA) program.

References

1. J. W. Goodman, *Introduction to Fourier Optics* (McGraw-Hill, 1996).
2. P. D. Foote, G. M. Proudley, G. S. Beddard, G. G. McFadyen, G. D. Reid, L. M. Connors, M. Bell, T. J. Hall, and K. Powell, Appl. Opt. **32**, 174 (1993).
3. C. Halvorson, A. Hays, B. Kraabel, R. Wu, F. Wudl, and A. J. Heeger, Science **265**, 1215 (1994).
4. A. A. Maznev, K. A. Nelson, and J. A. Rogers, Opt. Lett. **23**, 1319 (1998).
5. G. D. Goodno, G. Dadusc, and R. J. D. Miller, J. Opt. Soc. Am. B **15**, 1791 (1998).
6. S.-Y. Tseng, W. Cao, Y.-H. Peng, J. M. Hales, S.-H. Chi, J. W. Perry, S. R. Marder, C. H. Lee, W. N. Herman, and J. Goldhar, Opt. Express **14**, 8737 (2006).
7. J. A. Shirley, R. J. Hall, and A. C. Eckbreth, Opt. Lett. **5**, 380 (1980).
8. A. A. Maznev, T. F. Crimmins, and K. A. Nelson, Opt. Lett. **23**, 1378 (1998).
9. G. Ramos-Ortiz, M. Cha, S. Thayumanavan, J. C. Mendez, S. R. Marder, and B. Kippelen, Appl. Phys. Lett. **82**, 179 (2004).
10. G. Ramos-Ortiz, M. Cha, G. Walker, S. R. Marder, and B. Kippelen, in *Conference on Lasers and Electro-Optics/International Quantum Electronics Conference and Photonic Applications Systems Technologies*, Technical Digest (CD) (Optical Society of America, 2004), paper CTuZ7.
11. G. Ramos-Ortiz, M. Cha, B. Kippelen, G. A. Walker, S. Barlow, and S. R. Marder, Opt. Lett. **29**, 2515 (2004).
12. G. Ramos-Ortiz, Ph.D. dissertation (University of Arizona, 2003).
13. M. Samoc, A. Samoc, and B. Luther-Davies, Opt. Express **11**, 1787 (2003).